Organization of cytoplasmic domains of sarcoplasmic reticulum Ca^{2+}-ATPase in E_1P and E_1ATP states: a limited proteolysis study

Stefania Danko[a], Kazuo Yamasaki[a], Takashi Daiho[a], Hiroshi Suzuki[a,*], Chikashi Toyoshima[b]

[a] *Department of Biochemistry, Asahikawa Medical College, Midorigaokahigashi, Asahikawa 078-8510, Japan*
[b] *Institute of Molecular and Cellular Biosciences, The University of Tokyo, Bunkyo-ku, Tokyo 113-0032, Japan*

Received 12 July 2001; accepted 6 August 2001

First published online 22 August 2001

Edited by Vladimir Skulachev

Abstract In order to characterize the domain organization of sarcoplasmic reticulum Ca^{2+}-ATPase in different physiological states, limited proteolysis using three proteases (proteinase K (prtK), V8 and trypsin) was conducted systematically and quantitatively. The differences between E_2 and E_2P were examined in our previous study and E_2P was characterized by the complete resistance to all three proteases (except for trypsin attack at the very top of the molecule (T1 site)). The same strategies were employed in this study for E_1ATP, E_1PADP and E_1P states. Because of the transient nature of these states, they were either stabilized by non-hydrolyzable analogues or made predominant by adjusting buffer conditions. Aluminum fluoride (without ADP) was found to stabilize E_1P. All these states were characterized by strong (E_1ATP) to complete (E_1PADP and E_1P) resistance to prtK and to V8 but only weak resistance to trypsin at the T2 site. Because prtK and V8 primarily attack the loops connecting the A domain to the transmembrane helices whereas the trypsin T2 site (Arg^{198}) is located on the outermost loop in the A domain, these results lead us to propose that the A domain undergoes a large amount of rotation between E_1P and E_2P. Combined with previous results, we demonstrated that four states can be clearly distinguished by the susceptibility to three proteases, which will be very useful for establishing the conditions for structural studies.

Key words: Ca^{2+}-ATPase; P-type ion transporting ATPase; Ca^{2+} pump; Sarcoplasmic reticulum; Phosphorylated intermediate; Proteolysis

1. Introduction

Sarcoplasmic reticulum (SR) Ca^{2+}-ATPase is a 110 kDa membrane protein and a representative member of P-type ion transporting ATPases. It catalyzes Ca^{2+} transport coupled with ATP hydrolysis [1,2]. According to the E_1/E_2 theory, the enzyme with bound Ca^{2+} (E_1) is autophosphorylated by ATP bound at the catalytic site to form ADP-sensitive phosphoenzyme (E_1P). This phosphorylation causes the bound Ca^{2+} ions to be occluded at the transport sites, and the subsequent conformational transition to the ADP-insensitive form (E_2P) releases Ca^{2+} into the lumen. Finally, dephosphorylation takes place and returns the enzyme into the unphosphorylated and Ca^{2+}-unbound E_2 form (for recent reviews, see [3,4]).

Ca^{2+}-ATPase has three cytoplasmic domains (A, N and P), which are widely separated in the crystal structure with bound Ca^{2+} ([5], CaE_1 in Fig. 1). It has been proposed that when Ca^{2+} is absent, three cytoplasmic domains gather to form a single headpiece. This was based on the modeling of the enzyme in tubular crystals formed in the presence of decavanadate and in the absence of Ca^{2+} ([5], E_2V in Fig. 1). Then, an obvious and important issue to be addressed now is in which steps in the catalytic cycle such large domain movements take place. We would like to know if the movement of A domain is co-ordinated with the movement of N domain, and if the binding of ATP itself affects the domain organization. To answer these questions we believe that, although very classic, limited proteolysis is useful, because these proteases cleave quite distinct sites (Fig. 1). Proteinase K (prtK) cleaves primarily the loops connecting A domain to M2 and M3 transmembrane helices [6], V8 the loop connecting A domain to M3 helix [7]; trypsin attacks the outermost loop of A domain (T2 site) in addition to the loop at the top of N domain (T1 site) [8]. We first studied the difference between E_2 and E_2P [10] and demonstrated that E_2P is characterized by the complete resistance to all the three proteases (except for trypsin attack at T1 site). Because of the same resistance properties, the enzyme in the tubular crystals (E_2V) was identified to be in a state very close to E_2P. These results provided a strong support for the proposal that A domain rotates a large amount, because the protection of T2 site by P domain requires a nearly 90° rotation of A domain.

We now extend the same strategies to E_1ATP complex and E_1P to complete the characterization by limited proteolysis of various states in the catalytic cycle. The design of the experiments is as follows. Although it is impossible to stop the reaction in E_1ATP state, we could use non-hydrolyzable analogues (adenosine 5′-(β,γ-methylene)triphosphate (AMPPCP) in this study) to mimic E_1ATP; the effect of γ-phosphate can be addressed by comparing with ADP. 2′,3′-*O*-(2,4,6-Trinitrocyclohexadienylidene) (TNP)-AMP and TNP-ATP may also be useful for deciphering the effects of different parts of ATP. The E_1PADP state can be made with $Al^{3+}/F^-/ADP$ [11]. We also show that Al^{3+}/F^- alone (without ADP) stabilizes E_1P. The E_1P to E_2P transition can be blocked partially by adding a high concentration of Ca^{2+} or completely by using *N*-ethylmaleimide (NEM)-treated specimen [12]. We report here that

*Corresponding author. Fax: (81)-166-68 2359.
E-mail address: hisuzuki@asahikawa-med.ac.jp (H. Suzuki).

Abbreviations: SR, sarcoplasmic reticulum; E_1P, ADP-sensitive phosphoenzyme; E_2P, ADP-insensitive phosphoenzyme; prtK, proteinase K; AMPPCP, adenosine 5′-(β,γ-methylene)triphosphate; AMPPNP, adenosine 5′-(β,γ-imido)triphosphate; TNP, 2′,3′-*O*-(2,4,6-trinitrocyclohexadienylidene); NEM, *N*-ethylmaleimide

0014-5793/01/$20.00
PII: S0014-5793(01)02801-0

E_1P and E_1ATP have similar patterns of susceptibility, but distinctly different from those examined previously, including E_2P [10]. Taken altogether, we can now distinguish four states unequivocally by limited proteolysis. The results also indicate that the large rotation of A domain will take place between E_1P and E_2P.

2. Materials and methods

2.1. Preparation of SR vesicles and treatment with NEM

SR vesicles were prepared from rabbit skeletal muscle as described previously [13]. The content of phosphorylation site determined with $^{32}P_i$ according to Barrabin et al. [14] was 5.0 ± 0.2 nmol/mg of vesicle protein ($n = 6$). The Ca^{2+}-dependent ATPase activity determined at 25°C as described previously [13] was 2.51 ± 0.05 μmol/min/mg of vesicle protein ($n = 3$). SR vesicles were treated with NEM in the presence of adenosine 5′-(β,γ-imido)triphosphate (AMPPNP) according to Kawakita et al. [12]. The content of phosphorylation site was unaffected and the Ca^{2+}-dependent ATPase activity was completely suppressed by this treatment due to blocking of the E_1P to E_2P transition [12,15]. The NEM-treated vesicles were used in some proteolysis experiments with ATP.

2.2. Proteolysis of SR vesicles

SR vesicles (0.3 mg/ml of vesicle protein) were digested with prtK, V8 protease, or trypsin in a buffer containing 0.1 M KCl, 7 mM $MgCl_2$, 0.5 mM $CaCl_2$ plus 0.4 mM EGTA (0.103 mM Ca^{2+} at pH 6.7) or 20 mM $CaCl_2$ without EGTA, and 50 mM 3-(*N*-morpholino)-propanesulfonic acid/Tris (pH 6.7) or 50 mM 2-(*N*-morpholino)ethanesulfonic acid/Tris (pH 6.0), as stated in the legends for figures and tables. The concentration (mg/ml) of the protease and temperature were 0.05 (pH 6.7) or 0.1 (pH 6.0) and 25°C for the prtK proteolysis, 0.065 (pH 6.7 and pH 6.0) and 37°C for the V8 proteolysis, and 0.03 (pH 6.7) or 0.1 (pH 6.0) and 25°C for the tryptic proteolysis, respectively. For the V8 proteolysis, octaethylene glycol monododecyl ether at a non-solubilizing low concentration of 0.05 mg/ml was included in the reaction mixture as described previously [7]. Effects of ATP and its analogues were examined with ATP (± 5 mM), AMPPCP (± 1 mM), ADP (± 100 μM), TNP-AMP (± 10 μM) and TNP-ATP (± 10 μM), unless otherwise stated. ATP was added 5 s before the start of the proteolysis, and other nucleotides 5 min before the start. When the effects of $Al^{3+}/F^-/ADP/Mg^{2+}$ were examined, SR vesicles were pre-incubated essentially according to Troullier et al. [11] with $AlCl_3$ (± 50 μM), KF (± 3 mM), ADP (± 100 μM) and $MgCl_2$ (± 7 mM) for 40 min at 22°C and pH 6.7 in the presence of 0.1 mM Ca^{2+}, and then the proteolysis was started.

Proteolysis was terminated by adding ice-cold trichloroacetic acid to 2.5% (w/v) and diluting three times with a modified Laemmli sample buffer containing 3% (w/v) sodium dodecyl sulfate (SDS). 20 μl of each sample thus obtained was loaded on a 10.5% gel for SDS–polyacrylamide gel electrophoresis according to Laemmli [16]. For better resolution of the peptides on SDS gels, 1 mM $CaCl_2$ was included in both the stacking and separating gels for the V8- and prtK-treated samples [7]. The gels were stained by Coomassie brilliant blue R-250, and subjected to densitometric analysis with a GT9500-GT95FLU flatbed scanner (Epson, Tokyo, Japan) and Scion Image software (Scion Corp., Frederick, MD, USA).

2.3. Miscellaneous methods

V8 protease, prtK, trypsin (L-1-tosylamido-2-phenylethyl chloromethyl ketone-treated) were obtained from Sigma. AMPPCP and AMPPNP were also from Sigma. TNP-AMP and TNP-ATP were synthesized according to Hiratsuka [17]. Protein concentrations were determined by the method of Lowry et al. [18] with bovine serum albumin as a standard. Data were analyzed by non-linear regression using the program Origin (Microcal Software, Inc., Northampton, MA, USA).

3. Results

3.1. Degradation of SR Ca^{2+}-ATPase by proteases

Proteolysis of SR Ca^{2+}-ATPase in the presence of Ca^{2+} was carried out using prtK, V8 protease and trypsin to examine the effects of ATP, AMPPCP, ADP, TNP-AMP, TNP-ATP, Al^{3+}, F^- and Mg^{2+}. Typical digestion patterns with prtK and trypsin are shown in Fig. 2. The degradation of the 110 kDa ATPase chain with prtK measured by densitometric scan of the SDS gels was well approximated by first order reaction

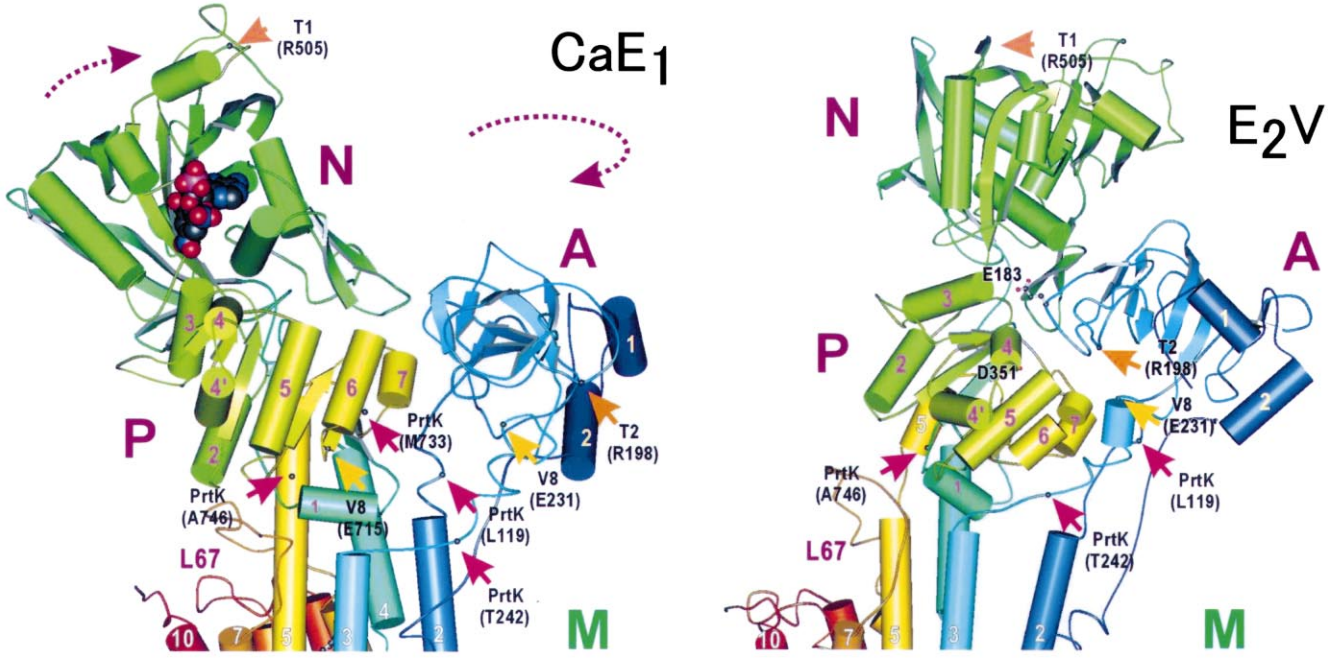

Fig. 1. Location of proteolytic cleavage sites on SR Ca^{2+}-ATPase. The positions of the main digestion sites by prtK [6], V8 [7] and trypsin [8] are shown on the atomic model of Ca^{2+}-ATPase [5] with bound Ca^{2+} (CaE_1; PDB accession code 1EUL) and that made for the decavanadate-bound form in the absence of Ca^{2+} (E_2V; PDB accession code 1FQU), which is analogous to E_2P [10]. The arrows in broken lines show the movements of A and N domains required to fit the atomic model of the Ca^{2+}-bound state (CaE_1) to that of E_2V.

Table 1
Effects of AMPPCP, ADP, TNP-AMP and TNP-ATP on the degradation rate of SR Ca^{2+}-ATPase

Protease	Relative rate constant (%)				
	No ligands	AMPPCP	ADP	TNP-AMP	TNP-ATP
PrtK	100	15 (36)	100	70	70
V8 protease	100	9 (7)	90	102	104
Trypsin (T2)	100	63 (89)	85	79	128

SR vesicles were digested with prtK, V8 and trypsin at pH 6.7 in the presence of Ca^{2+} (0.1 mM), Mg^{2+} (7 mM) and nucleotides, as described in Section 2. The rate constants given are those for the degradation of the 110 kDa Ca^{2+}-ATPase polypeptide chain (prtK and V8) and those for the formation of A1 fragment (trypsin, cleavage at Arg^{198} (T2)). The numbers were obtained by least-squares fit as described in Fig. 2 and given in percentages to those obtained in the absence of nucleotides (no ligands). The numbers in parentheses show the rates in the presence of AMPPCP but in the absence of Mg^{2+}; they were normalized to the rates in the absence of both AMPPCP and Mg^{2+} (100%). The results obtained with AMPPCP at 3 mM, ADP at 0.5 mM, and TNP-AMP and TNP-ATP at 30 (and 3) μM (data not shown) were almost the same as those listed above obtained with AMPPCP at 1 mM, ADP at 0.1 mM, and TNP-AMP and TNP-ATP at 10 μM, respectively.

kinetics (Fig. 2A,C). In all the trypsin digestion experiments, the cleavage at T1 site (Arg^{505}) was very rapid and produced A and B fragments. The formation of the C-terminal A1 fragment upon further cleavage of A fragment at the T2 site (Arg^{198}) and its subsequent degradation were well described by consecutive first order reaction kinetics (Fig. 2B,D). All the major digestion products by prtK, V8 and trypsin were found to be consistent with those published previously [6–9,19–22]. Only the relative rate constants for the degradation of 110 kDa ATPase chain (prtK and V8 proteolysis) and those for the formation of A1 fragment (trypsin proteolysis) are therefore listed in Tables 1–3. Table 1 summarizes the effects of nucleotide binding. The numbers for stable E_1P analogues are given in Table 2. Table 3 summarizes the experiments with ATP.

3.2. Effects of nucleotides on digestion of SR Ca^{2+}-ATPase

The effects of nucleotide binding to Ca^{2+}-ATPase in the presence of 0.1 mM Ca^{2+} and 7 mM $MgCl_2$ were examined with AMPPCP, ADP, TNP-AMP and TNP-ATP (Table 1). AMPPCP, a non-hydrolyzable ATP analogue that will fix the enzyme in the E_1ATP state [13,23–25], was clearly different from others. Only AMPPCP provided strong resistance against prtK and V8, and protected A1, A2 and B tryptic fragments from further degradation. TNP-ATP did not show such protection effects. On the other hand, none of the nucleotides provided strong resistance to trypsin cleavage at the T2 site, although AMPPCP somewhat slowed down the degradation process. TNP-ATP even accelerated the degradation. Thus the γ-phosphate was essential for these protections but the TNP moiety impaired them.

3.3. Effects of Al^{3+}, F^-, ADP and Mg^{2+} on digestion of SR Ca^{2+}-ATPase

Aluminum fluorides (AlF_3 and AlF_4^-) have been used widely as γ-phosphate analogues for ATPases and GTPases [11,26–29]. With Ca^{2+}-ATPase, Troullier et al. [11] demonstrated that AlF_4^- and ADP make a stable complex with the enzyme in the presence of Ca^{2+} and Mg^{2+}, presumably fixing the enzyme in E_1PADP, the state immediately after phosphorylation with ATP. Digestion experiments with this complex showed complete resistance to prtK and to V8, but only a weak resistance to trypsin (Table 2). We then examined the protection effects for all the possible combinations of the four components (i.e. Al^{3+}, F^-, ADP, Mg^{2+}), and found that Al^{3+}/F^-/ADP (no Mg^{2+}) and Al^{3+}/F^-/Mg^{2+} were also equally effective. Hence we consider that the complex of Ca^{2+}-ATPase with Al^{3+}/F^-/ADP represents E_1PADP whereas Al^{3+}/F^-/Mg^{2+} represents E_1P and that they have similar compact domain organizations. Judging from the digestion rates of the 110 kDa ATPase chain and those at the tryptic T2 site, the domain organizations in E_1PADP and E_1P are close to that in E_1ATP, but distinctly different from that in E_2P (completely resistant to trypsin attack at the T2 site [10]).

3.4. Effects of ATP on digestion of SR Ca^{2+}-ATPase

To make the enzyme predominantly in the E_1P state with the natural substrate (ATP), we tried two ways. The first was to add 20 mm Ca^{2+} (in the presence of K^+) so that the transition from E_1P to E_2P is largely blocked; low pH (pH 6) was chosen to avoid too rapid exhaustion of ATP. As expected, nearly complete protection was found against prtK and V8 (Table 3). The second was to use NEM-treated specimen with which the E_1P to E_2P transition is completely blocked [12,15]. With this specimen, complete protection against prtK and V8 was observed even at pH 6.7 and low Ca^{2+} concentration (0.1 mM).

4. Discussion

As described, E_1ATP, E_1PADP and E_1P states of SR Ca^{2+}-ATPase can now be characterized by a strong resistance to

Table 2
Effects of Al^{3+}, F^- and ADP on the degradation rate of SR Ca^{2+}-ATPase

Protease	Relative rate constant (%)							
	No ligands	Al^{3+}/F^-/ADP	Al^{3+}/F^-	Al^{3+}/ADP	ADP/F^-	F^-	Al^{3+}	ADP
PrtK	100	2, 0 (1)	8 (56)	93	60	101	111	100
V8 protease	100	0 (0)	0 (83)	101	70	50	108	90
Trypsin (T2)	100	71 (76)	64 (125)	100	68	87	93	85

SR vesicles were treated with the ligands (Al^{3+}, F^- and ADP) at pH 6.7 in the presence of Ca^{2+} (0.1 mM) and Mg^{2+} (7 mM), and then digested with prtK, V8 and trypsin, as described in Section 2. Refer to Table 1 for the meaning of the 'relative rate constant'. The numbers in parentheses show the degradation rates in the presence of the ligands but in the absence of Mg^{2+}; they were normalized to the rates in the absence of both the ligands and Mg^{2+} (100%).

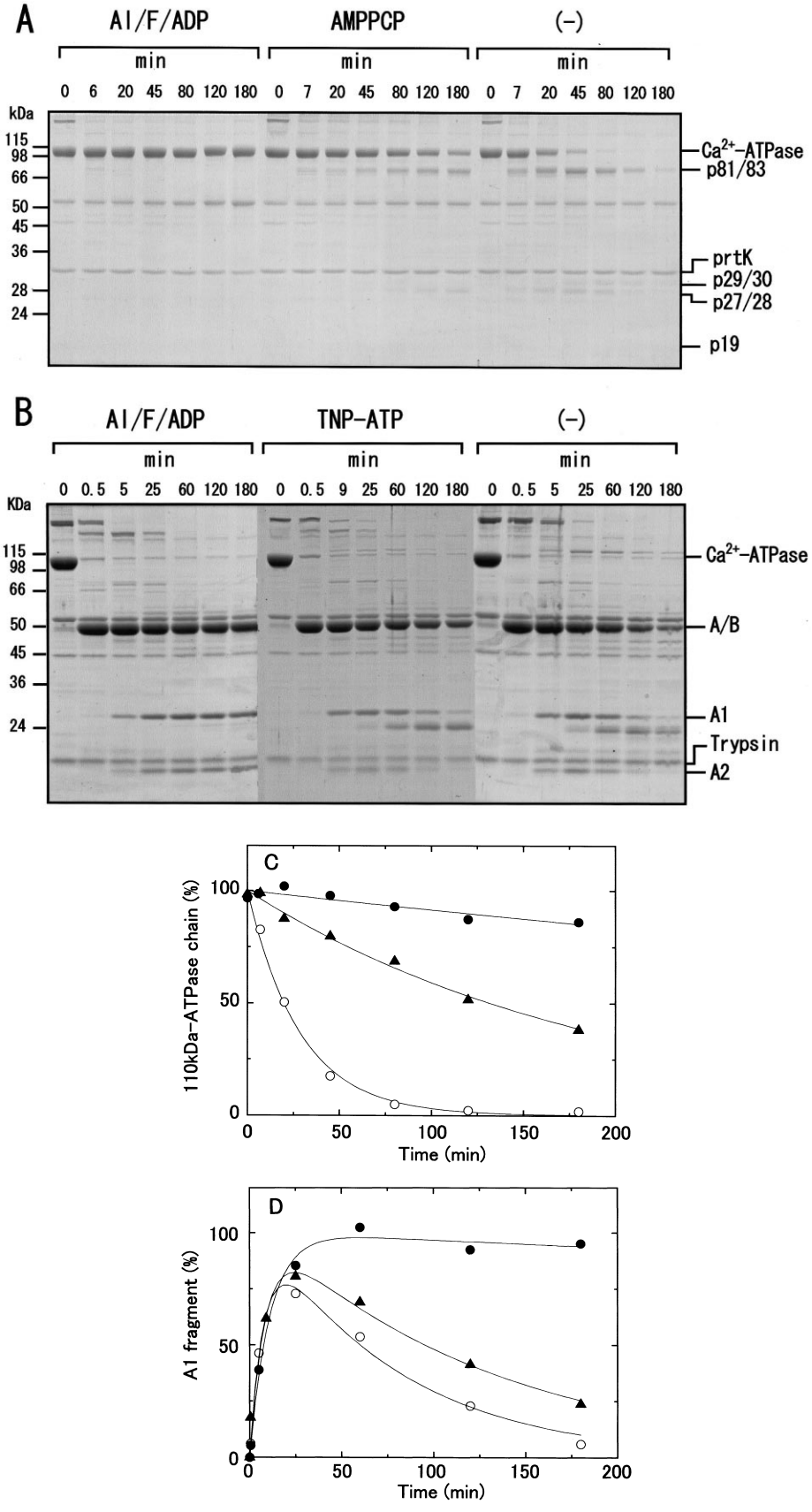
A
Al/F/ADP
AMPPCP
(−)
min
0 6 20 45 80 120 180 0 7 20 45 80 120 180 0 7 20 45 80 120 180
kDa
115
98
66
50
45
36
28
24
Ca2+-ATPase
p81/83
prtK
p29/30
p27/28
p19
B
Al/F/ADP
TNP-ATP
(−)
min
0 0.5 5 25 60 120 180 0 0.5 9 25 60 120 180 0 0.5 5 25 60 120 180
KDa
115
98
66
50
45
36
24
Ca2+-ATPase
A/B
A1
Trypsin
A2
C
110kDa-ATPase chain (%)
100
50
0
0 50 100 150 200
Time (min)
D
A1 fragment (%)
100
50
0
0 50 100 150 200
Time (min)

Fig. 2. Effects of AMPPCP, TNP-ATP and Al^{3+}/F^{-}/ADP on the prtK and trypsin digestion of SR Ca^{2+}-ATPase. SR vesicles treated with Al^{3+}, F^{-} and ADP (Al/F/ADP), and untreated vesicles preincubated with AMPPCP (AMPPCP) and TNP-ATP (TNP-ATP) or without those ligands (−), were digested with prtK (A, C) and trypsin (B, D) in the presence of 7 mM Mg^{2+} and 0.1 mm Ca^{2+} at pH 6.7, as described in Section 2. A: SDS gels of the prtK digests, and (B) those of the trypsin digests. The positions of Ca^{2+}-ATPase and its proteolytic fragments, and those of the molecular mass markers are indicated on the right and the left margins, respectively. C: The time courses for the amounts of the 110 kDa Ca^{2+}-ATPase polypeptide chain in prtK digestion with the Al^{3+}/F^{-}/ADP-treated (●) and untreated (○, ▲) vesicles in the absence (○) or presence (▲) of AMPPCP. D: The time courses for the amounts of A1 fragment in trypsin digestion with the Al^{3+}/F^{-}/ADP-treated (●) and untreated (○, ▲) vesicles in the absence (○) or presence (▲) of TNP-ATP. Solid lines in (C) show least-squares fit of a single exponential to the time course for the amounts of the 110 kDa ATPase chain, in which the first order rate constants (h^{-1}) were 0.053 for the Al^{3+}/F^{-}/ADP-treated vesicles, 2.1 for the untreated vesicles, and 0.32 for the untreated vesicles in the presence of AMPPCP. Solid lines in (D) show least-squares fit of a double exponential in a consecutive formation and decay reaction to the time course for the amounts of A1 fragment, in which the formation rate constants and decay rate constants (h^{-1}) were 5.5 and 0.022 for the Al^{3+}/F^{-}/ADP-treated vesicles, 7.7 and 0.80 for the untreated vesicles, and 7.1 and 0.48 for the untreated vesicles in the presence of TNP-ATP.
←

prtK and to V8 but a weak resistance to trypsin at the T2 site. This is in marked contrast with E_2P, which is characterized by complete resistance to all of these [10]. The protection against prtK and V8 was somewhat less in E_1ATP stabilized by AMPPCP than in E_1P. This difference will probably be explained by the equilibrium between E_1 and E_1AMPPCP, considering that digestion proceeds irreversibly if the population of enzyme in E_1 state exists at all. Thus, combined with our previous results [10], four states in the reaction cycle (E_1, E_1ATP or E_1P, E_2P and E_2) can be distinguished by their characteristic differences in the susceptibilities to three proteases, which can be quantitated simply by relative digestion rates (Table 4).

Then the question is how these proteolysis results can be interpreted in the light of three-dimensional (3D) structure. Can we consider in a simple minded way that the decreases in degradation rate constants represent the steric blocks of the cleavage sites? Of course we cannot exclude the possibility that conformational changes unrelated to domain movements altered the susceptibility of the cleavage sites. However, 3D structure modeled for vanadate-induced tubular crystals ([5], E_2V in Fig. 1; analogous to E_2P) and that determined for Mg^{2+}/F^{-} complex (a stable E_2P analogue [30–33]; Toyoshima et al., unpublished results) showed that all the cleavage sites are blocked sterically by gathering of all three cytoplasmic domains. Hence in the following discussion, we simply relate the protection effects with steric blocking due to domain movements schematized in Fig. 3.

The simplest interpretation of the observed protections in E_1ATP and E_1P is that N and P domains are in closed configuration crosslinked by ATP (having adenosine on one end and γ-phosphate on the other end), by Al^{3+}/F^{-}/ADP or $Al^{3+}/F^{-}/Mg^{2+}$ (presumably due to strong interaction of fluoride with amide nitrogen), or by phosphate covalently bound to Asp^{351}. Absolute requirement of γ-phosphate for the protection was evident, because ADP showed no effect for the primary cleavage site (Glu^{243}) (Table 1). Also reported was a protection by AMPPNP, another non-hydrolyzable ATP analogue, of A1 and A2 tryptic fragments from further degradation [20]. Bidentate β,γ-CrATP, which stabilizes the Ca^{2+}-occluded state (analogous to E_1P) [34], conferred resistance to prtK [35] but not to trypsin [21]. It is understandable that the TNP moiety impaired the protection effects, because TNP-ATP is virtually non-hydrolyzable with Ca^{2+}-ATPase [36,37]. Presumably, the TNP moiety, which provides much higher affinity for TNP-ATP than ATP [38,39], prevents proper binding of the ATP moiety to the enzyme and positioning of γ-phosphate.

Table 3
Effects of ATP on the degradation rate of SR Ca^{2+}-ATPase

Protease	Relative rate constant (%)		
	No ATP	Native SR	NEM-modified SR
PrtK	100	5 (22)	0 (1)
V8 protease	100	2	0[a] (12[a])
Trypsin (T2)	100	68	ND

Effects of ATP on prtK, V8 and trypsin digestion of the unmodified (native SR) and NEM-modified (NEM-modified SR) Ca^{2+}-ATPases were examined at pH 6.0 in the presence of 20 mm $CaCl_2$, or 0.5 mm $CaCl_2$ plus 0.4 mm EGTA (the numbers in parentheses), as described in Section 2. Refer to Table 1 for the meaning of the 'relative rate constant'. ND: not determined.
[a]Determined at pH 6.7.

Because the adenosine moiety of ATP is considered to bind around Phe^{487} in N domain and because the phosphorylation site (Asp^{351}) on P domain is distant by ∼25 Å in the crystal structure of the Ca^{2+}-bound (E_1) state [5], very large motion of domain closure is necessary for the γ-phosphate to reach the phosphorylation site. In the model for the vanadate-induced tubular crystals (E_2V in Fig. 1; analogous to E_2P), N domain is closer to P domain by ∼20° compared to that in the E_1 state; this amount is still too small for bringing the γ-phosphate to Asp^{351}. This is also true for glutaraldehyde crosslinking, which is most reactive in E_1P but unreactive in E_2P, between Lys^{492} in N domain and Arg^{678} in P domain [40]. Therefore, in the E_1ATP and in E_1P form, N domain may come even closer to P domain than in the E_2V (E_2P) form (Fig. 3).

Then, it is likely that, in E_1ATP and E_1P, A domain does not come to the position in which A and N domains can make several hydrogen bonds to stabilize the interaction between them as in E_2P. This view is totally consistent with the observation that the T2 site on A domain is rapidly cleaved in E_1ATP and E_1P, but completely resistant in E_2P. Therefore, a large motion of A domain, i.e. rotation by ∼90°, and its strong association with P and N domains occur most likely during the E_1P to E_2P transition (Fig. 3).

The large motion of domain closure of N and P domains in E_1ATP and E_1P will inevitably cause distortion in P domain, at least in the half closer to N domain. In fact, fluorescence from EDANS attached to Cys^{674} in that half of P domain changes greatly on the formation of E_1ATP (and only slightly by going further into E_1P) [23–25,41]. The distortion will likely cause the movement of M3 and the loop connecting A domain (possibly through the hydrogen bond between Glu^{340} on Pα1 and Thr^{247} (see figure 8 in [5]), or through the interaction with the loop connecting M6 and M7 because the mutations there slow down the phosphorylation [42]).

Then, 'in E_1ATP and E_1P, does A domain occupy a posi-

Table 4
Relative digestion rates for the intermediates in the catalytic cycle of SR Ca^{2+}-ATPase

Protease	Primary cleavage sites	Relative rate constant (%)						
		E_2[b] (no ligands)	E_1[a,b] (Ca^{2+})	E_1ATP[a] (AMPPCP)	E_1PADP[a] ($Al^{3+}/F^-/ADP$)	E_1P[a] ($Al^{3+}/F^-/Mg^{2+}$, ATP)	E_2P[b] (Mg^{2+}/F^-, orthovanadate)	E_2V[b] (decavanadate)
PrtK	L119(↓), T242(↑), M733/A746	100	113	17	0	0	1	0
V8 protease	E231(↑), E715(↓)	100	107	10	0	0	0	0
Trypsin (T2)	R198(↑)	100	211	133	150	135	0	0

The representative numbers for digestion rates obtained in our present and previous [10] studies for the six major intermediates (E_2, E_1, E_1ATP, E_1PADP, E_1P, and E_2P) in the catalytic cycle of Ca^{2+}-ATPase were summarized together with those for the decavanadate-bound state without Ca^{2+} (E_2V), which forms the tubular crystals [46]. The ligands used for stabilizing individual states are shown in parentheses. In the prtK and V8 digestion, the rate constants for the degradation of the 110 kDa Ca^{2+}-ATPase polypeptide chain were shown. In the trypsin digestion, the rate constants for the cleavage at Arg^{198} (T2) were shown. The rate constants were normalized to that obtained in the absence of Ca^{2+} and ligands (E_2 (no ligands)) (100%). The primary cleavage sites [6–8] were listed with their C-terminal residues: (↑) and (↓) indicate the increase and decrease, respectively, in the cleavage rate of the Ca^{2+}-bound state (E_1) compared to the unbound state (E_2).
[a]Data obtained in this study.
[b]Data obtained in our previous study [10].

tion different from that in E_1?' will be the next question. Probably so. The protection against trypsin attack in E_1ATP and E_1P states was far from complete (only to 2/3 in the rate constant) but significant. The complete protection against prtK in these states will imply that the loop connecting M3 and A domain has moved toward and is protected by P domain (Fig. 1). The complete protection against V8 means that the part (around Glu^{231}) of the same loop closer to A domain has also moved and that the part of P domain (including Glu^{715}) that makes contacts with the upper part of M3 has become inaccessible to the protease. Therefore, it is likely that, in E_1ATP and E_1P, A domain has moved toward P domain, but the domain is not yet rotated as in E_2P (Fig. 3).

These notions on the domain arrangements are in complete agreement with the results by Fe-catalyzed cleavage of Na^+,K^+-ATPase. Karlish and co-workers proposed using this technique [43] that A domain is not in close contact with P domain in E_1ATP and E_1P, but is so in E_2P. They showed that TGES sequence (starting from Thr^{181} with Ca^{2+}-ATPase) comes close to TGDGVND (starting from Thr^{701} with Ca^{2+}-ATPase) in E_2P. The location of T2 site (Arg^{198}) is very close to Glu^{183} in the 3D structure (Fig. 1; [5]).

All these data support the idea that cytoplasmic domains of Ca^{2+}-ATPase take distinctly different arrangements in the catalytic cycle, and show that they can be distinguished by limited proteolysis. The results also strongly suggest that the

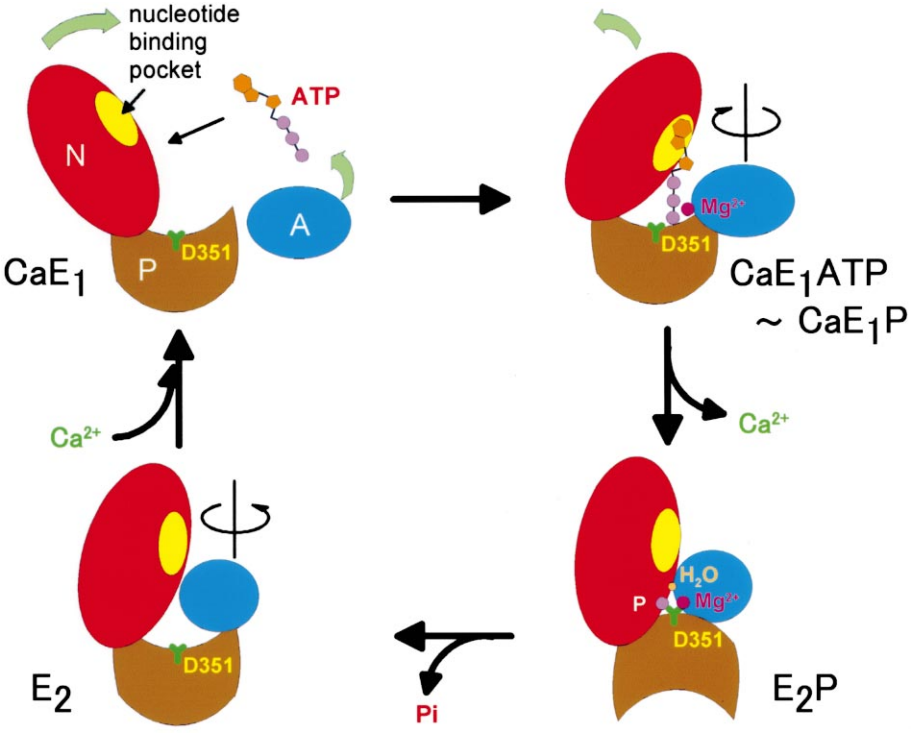

Fig. 3. Schematic models for four distinct arrangements of three cytoplasmic domains (N, P and A) in the catalytic cycle of Ca^{2+}-ATPase. Arrows indicate the proposed domain movements. In the text and tables, 'CaE_1' and 'CaE_1ATP' to 'CaE_1P' were described without 'Ca' for simplicity.

large rotation of A domain takes place during the E_1P to E_2P transition and this rearrangement is likely to be a key event in the whole reaction cycle. In fact, the enzyme cleaved at Glu^{231} by V8 can be phosphorylated by ATP but does not undergo normal enzymatic turnover (due to blocking of the E_1P to E_2P transition) [7]. This is also the case with the enzyme cleaved at Thr^{242} by prtK [9]. In the enzyme cleaved at T3b site (Lys^{234} or Arg^{236}) by trypsin, the E_1P to E_2P transition is blocked [22]. Mutations of Gly^{233}, which is highly conserved among P-type ATPases, result in a very slow transition of E_1P to E_2P [44]. Furthermore, glutaraldehyde-crosslinked enzyme, presumably fixed in an E_1ATP-like configuration, does not proceed from E_1P to E_2P [40]. All these data suggest that Ca^{2+}-ATPase utilizes A domain for realizing the hydrophobic atmosphere [45] around the phosphorylation site in E_2P state so that a specific water molecule can attack the acylphosphate (Fig. 3). Also the stabilization energy provided by intimate contacts between all three cytoplasmic domains in E_2P will provide energy for moving transmembrane helices and release bound Ca^{2+} ions.

Finally, for structural studies of intermediate states, it is vital to find conditions to stabilize them perfectly and efficient methods for examining how stable they are. The methods and conditions established in this (for E_1P) and our previous (for E_2P) [10] studies must be useful for making good crystals.

Acknowledgements: We thank Dr. Haruo Ogawa, University of Tokyo, for preparing Fig. 3. This work was supported by a grant-in-aid for scientific research from the Ministry of Education, Culture, Sports, Science and Technology, Japan (to H.S.).

References

[1] Ebashi, S. and Lipmann, F. (1962) J. Cell Biol. 14, 389–400.
[2] Hasselbach, W. and Makinose, M. (1961) Biochem. Z. 333, 518–528.
[3] MacLennan, D.H., Rice, W.J. and Green, N.M. (1997) J. Biol. Chem. 272, 28815–28818.
[4] Møller, J.V., Juul, B. and le Maire, M. (1996) Biochim. Biophys. Acta 1286, 1–51.
[5] Toyoshima, C., Nakasako, M., Nomura, H. and Ogawa, H. (2000) Nature 405, 647–655.
[6] Juul, B., Turc, H., Durand, M.L., Gomez de Gracia, A., Denoroy, L., Møller, J.V., Champeil, P. and le Maire, M. (1995) J. Biol. Chem. 270, 20123–20134.
[7] le Maire, M., Lund, S., Viel, A., Champeil, P. and Moller, J.V. (1990) J. Biol. Chem. 265, 1111–1123.
[8] Brandl, C.J., Green, N.M., Korczak, B. and MacLennan, D.H. (1986) Cell 44, 597–607.
[9] Juul, B. and Møller, J.V. (2000) in: Na/K-ATPase and Related ATPases (Taniguchi, K. and Kaya, S., Eds.), pp. 233–236, Elsevier, Amsterdam.
[10] Danko, S., Daiho, T., Yamasaki, Y., Kamidochi, M., Suzuki, H. and Toyoshima, C. (2001) FEBS Lett. 489, 277–282.
[11] Troullier, A., Girardet, J.-L. and Dupont, Y. (1992) J. Biol. Chem. 267, 22821–22829.
[12] Kawakita, M., Yasuoka, K. and Kaziro, Y. (1980) J. Biochem. (Tokyo) 87, 609–617.
[13] Nakamura, S., Suzuki, H. and Kanazawa, T. (1994) J. Biol. Chem. 269, 16015–16019.
[14] Barrabin, H., Scofano, H.M. and Inesi, G. (1984) Biochemistry 23, 1542–1548.
[15] Suzuki, H. and Kanazawa, T. (1995) J. Biol. Chem. 270, 3089–3093.
[16] Laemmli, U.K. (1970) Nature 227, 680–685.
[17] Hiratsuka, T. (1982) Biochim. Biophys. Acta 719, 509–517.
[18] Lowry, O.H., Rosebrough, N.J., Farr, A.L. and Randall, R.J. (1951) J. Biol. Chem. 193, 265–275.
[19] Dux, L. and Martonosi, A. (1983) J. Biol. Chem. 258, 10111–10115.
[20] Imamura, Y., Saito, K. and Kawakita, M. (1984) J. Biochem. (Tokyo) 95, 1305–1313.
[21] Andersen, J.P., Vilsen, B., Collins, J.H. and Jørgensen, P.L. (1986) J. Membr. Biol. 93, 85–92.
[22] Imamura, Y. and Kawakita, M. (1989) J. Biochem. (Tokyo) 105, 775–781.
[23] Kubo, K., Suzuki, H. and Kanazawa, T. (1990) Biochim. Biophys. Acta 1040, 251–259.
[24] Suzuki, H., Nakamura, S. and Kanazawa, T. (1994) Biochemistry 33, 8240–8246.
[25] Kanazawa, T., Suzuki, H., Daiho, T. and Yamasaki, K. (1995) Biosci. Rep. 15, 317–326.
[26] Coleman, D.E., Berghuis, A.M., Lee, E., Linder, M.E., Gilman, A.G. and Sprang, S.R. (1994) Science 265, 1405–1412.
[27] Sondek, J., Lambright, D.G., Noel, J.P., Hamm, H.E. and Sigler, P.B. (1994) Nature 372, 276–279.
[28] Fisher, A.J., Smith, C.A., Thoden, J.B., Smith, R., Sutoh, K., Holden, H.M. and Rayment, I. (1995) Biochemistry 34, 8960–8972.
[29] Braig, K., Menz, R.I., Montgomery, M.G., Leslie, A.G.W. and Walker, J.E. (2000) Structure 8, 567–573.
[30] Murphy, A.J. and Coll, R.J. (1992) J. Biol. Chem. 267, 5229–5235.
[31] Murphy, A.J. and Coll, R.J. (1992) J. Biol. Chem. 267, 16990–16994.
[32] Kubota, T., Daiho, T. and Kanazawa, T. (1993) Biochim. Biophys. Acta 1163, 131–143.
[33] Daiho, T., Kubota, T. and Kanazawa, T. (1993) Biochemistry 32, 10021–10026.
[34] Vilsen, B. and Andersen, J.P. (1992) J. Biol. Chem. 267, 3539–3550.
[35] Møller, J.V., Ning, G., Maunsbach, A.B., Fujimoto, K., Asai, K., Juul, B., Lee, Y.-J., Gomez de Gracia, A., Falson, P. and le Maire, M. (1997) J. Biol. Chem. 272, 29015–29032.
[36] Watanabe, T. and Inesi, G. (1982) J. Biol. Chem. 257, 11510–11516.
[37] Dupont, Y., Pougeois, R., Ronjat, M. and Verjovsky-Almeida, S. (1985) J. Biol. Chem. 260, 7241–7249.
[38] Dupont, Y., Chapron, Y. and Pougeois, R. (1982) Biochem. Biophys. Res. Commun. 106, 1272–1279.
[39] Suzuki, H., Kubota, T., Kubo, K. and Kanazawa, T. (1990) Biochemistry 29, 7040–7045.
[40] McIntosh, D.B. (1992) J. Biol. Chem. 267, 22328–22335.
[41] Suzuki, H., Obara, M., Kubo, K. and Kanazawa, T. (1989) J. Biol. Chem. 264, 920–927.
[42] Zhang, Z., Lewis, D., Sumbilla, C., Inesi, G. and Toyoshima, C. (2001) J. Biol. Chem. 276, 15232–15239.
[43] Patchornik, G., Goldshleger, R. and Karlish, S.J.D. (2000) Proc. Natl. Acad. Sci. USA 97, 11954–11959.
[44] Andersen, J.P., Vilsen, B., Leberer, E. and MacLennan, D.H. (1989) J. Biol. Chem. 264, 21018–21023.
[45] de Meis, L., Martins, O.B. and Alves, E.W. (1980) Biochemistry 19, 4252–4261.
[46] Dux, L. and Martonosi, A. (1983) J. Biol. Chem. 258, 2599–2603.